Mobility of Dislocations in Aluminum*

J. A. GORMAN, D. S. WOOD, AND T. VREELAND, JR.
W. M. Keck Laboratories, California Institute of Technology, Pasadena, California 91109
(Received 15 August 1968)

The velocities of individual dislocations of edge and mixed types in pure aluminum single crystals were determined as a function of applied-resolved shear stress and temperature. The dislocation velocities were determined from measurements of the displacements of individual dislocations produced by stress pulses of known duration. The Berg–Barrett x-ray technique was employed to observe the dislocations, and stress pulses of 15 to 108 μsec duration were applied by propagating torsional waves along the axes of [111]-oriented cylindrical crystals. Resolved shear stresses up to 16×10^6 dynes/cm² were applied at temperatures ranging from −150° to +70°C, and dislocation velocities were found to vary from 10 to 2800 cm/sec over these ranges of stress and temperature. The experimental conditions were such that the dislocation velocities were not significantly influenced by impurities, dislocation curvature, dislocation-dislocation interactions, or long-range internal stress fields in the crystals. The velocity of dislocations is found to be linearly proportional to the applied-resolved shear stress, and to decrease with increasing temperature. Qualitative comparison of these results with existing theories leads to the conclusion that the mobility of individual dislocations in pure aluminum is governed by dislocation-phonon interactions. The phonon-viscosity theory of dislocation mobility can be brought into agreement with the experimental results by reasonable choices of the values of certain constants appearing in the theory.

INTRODUCTION

Recent dislocation mobility measurements performed on two metals with close packed structures, copper[1] and zinc,[2] have shown that dislocation velocity on close packed planes is approximately linearly proportional to stress at room temperature, and exceeds 10^2 cm/sec at the macroscopic yield stress. These results are in approximate agreement with theories which assume that dislocation mobility is governed by dislocation–phonon interactions. The purpose of this investigation was to determine if dislocation mobility in aluminum, another metal with a close packed structure, also agrees with the predictions of the phonon-interaction theories; and, in particular, to determine if the temperature dependence of the dislocation velocity in aluminum is in agreement with these theories.

All tests were performed on 99.999% pure aluminum single crystals machined into right circular cylinders with [111] axes. Dislocations were produced on one end of each specimen by scratching with an Al_2O_3 whisker, or by damaging with a focused laser pulse. Dislocation motion was produced by subjecting the specimens to torsion stress pulses of a few μsec duration. Dislocation positions were observed before and after applying stress pulses using the Berg–Barrett x-ray technique.

TEST-SPECIMEN PREPARATION

Single aluminum crystals were grown using 99.999% pure aluminum. Crystals were grown in high-purity graphite molds under high vacuums (about 10^{-5} mm Hg), using a technique similar to that described by Young.[3] The molds were made of grade AUC graphite, coated with colloidal graphite and baked at 150°C in air before installing the aluminum charge.

A crystal was also grown by a soft-mold technique similar to that described by Noggle,[4] except that a helium atmosphere was used rather than high vacuum. It was necessary to bake the aluminum charge and alumina mold powder at 600°C for about 24 h under mechanical-pump vacuum before growing the crystal, in order to prevent the formation of bubbles in the aluminum.

The best crystals produced in the graphite molds contained subgrains of 3 or 4 mm diam after a one-hour anneal at 630°C. The crystal grown by the soft mold technique required about two weeks of annealing while cycling the temperature between 480° and 635°C once an hour to obtain comparable subgrain sizes.

Test specimens were cut from the as-grown crystals and machined into [111]-oriented right circular cylinders by spark machining. The cylindrical surface and the end on which dislocation motion was to be observed were electrolytically machined for a depth of at least 1.5 mm to remove the damage introduced by spark machining. The electrolyte used was 2 parts methanol and 1 part nitric acid. A current density of about 1 A/cm² was used for most of the electrolytic machining. If the surface had a thick oxide coating, it was found useful to use a current density of about 5 A/cm² for the first fifteen seconds to break down the oxide coating uniformly over the surface. Test specimens were reused several times. After testing, the observation surface was repolished by electrolytic machining.

After machining, the specimens were annealed for one hour at 630°C to remove all dislocations within the

* This work was supported by the U.S. Atomic Energy Commission.
[1] W. F. Greenman, T. Vreeland, Jr., and D. S. Wood, J. Appl. Phys. **38**, 3595 (1967).
[2] D. P. Pope, T. Vreeland, Jr., and D. S. Wood, J. Appl. Phys. **38**, 4011 (1967).
[3] F. W. Young and J. R. Savage, J. Appl. Phys. **35**, 1917 (1964).
[4] T. S. Noggle, Rev. Sci. Instr. **24**, 184 (1953).

depth observable by the Berg–Barrett x-ray technique (about 10 μ), except for those dislocations making up the subgrain boundaries. The atmosphere used for annealing was helium passed through an anhydrous $CaSO_4$ drying tower, and activated charcoal held at -196°C, or high purity argon passed through an anhydrous $CaSO_4$ drying tower.

EXPERIMENTAL TECHNIQUES

Methods for Producing Dislocations Near the Observation Surface

Dislocations were produced on (111) planes close to the observation surface by scratching the surface in a grid pattern in the $[11\bar{2}]$ and $[1\bar{1}0]$ directions. The scratching was done using an Al_2O_3 wisker mounted on an arm attached to a calibrated torsion wire. A load of 50 mg and a scratching speed of 9 cm/min were found to produce the best dislocations, i.e., with long lengths parallel to the scratch. Scratches in both the $[11\bar{2}]$ and $[1\bar{1}0]$ directions produced dislocations parallel to the scratches. Both edge type and mixed dislocations were produced by scratches in the $[11\bar{2}]$ direction. Mixed dislocations were produced by scratches in the $[1\bar{1}0]$ direction.

Laser pulses were also used to produce dislocations. A "giant" single pulse of energy from a ruby laser was focused to a 3-mm-long line on the specimen observation surface by means of a cylindrical lens. The width of the line was kept to about 0.02 mm by slits. The pulse duration was about 20 to 50 nsec and the energy incident on the specimen surface during one pulse was about 0.01 J. The energy actually absorbed by the specimen was not measured. Three or more pulses, spaced at ten minute intervals, were used at each damage location on the specimen. The damage lines were oriented radially on the test surface in $\langle 11\bar{2}\rangle$ directions. Dislocations nearly parallel to the damage line and of mainly edge character were produced.

X-ray Technique for Observing Dislocations

Dislocations on (111) planes near the observation surface of the specimen were observed using the Berg–Barrett x-ray technique described by Turner, Vreeland, and Pope.[5] Characteristic iron radiation from a Machlett A-2 diffraction tube operating at 50 kV and 7.5 mA was employed to obtain {220} reflections from the specimens. The reflected x-rays were recorded on Kodak high-resolution plates. The resolution obtained by this technique was about 10 μ.

The Burgers vector of a dislocation can be determined using the fact that contrast at a dislocation will be very low if $\mathbf{b}\cdot\mathbf{n}=0$, where $\mathbf{b}$ is the Burgers vector and $\mathbf{n}$ is the normal to the reflecting plane. There are three {220}-type reflecting planes suitable for taking Berg–Barrett x-ray micrographs of the (111) plane. By taking x-ray micrographs using all three reflecting planes, it is possible to determine the Burgers vectors of all the dislocations.

Loading System

The torsion machine described by Pope, Vreeland, and Wood[6] was employed to apply torque pulses of known amplitude and duration to the specimens. The machine generates a step-function-elastic-torsion wave front having a rise time of about 2 μsec. This wave front propagates successively through a polycrystalline aluminum gauge bar, the test specimen, and a polycrystalline extender bar, these three all being of the same diameter and bonded together at their ends, as shown in Fig. 1. The wave front then reflects as an unloading wave from the free end of the extender bar, and propagates in the reverse direction through the system. The observation surface of the specimen was located at the bond between the gauge bar and specimen. The machine is arranged so that only a single round-trip passage of the wave front through the specimen and extender bar occurs, subjecting the specimen to only a single torsion pulse.

Semi-conductor strain gauges bonded to the gauge bar 0.7 cm from the specimen observation surface, together with a suitable single sweep oscilloscope and recording camera, were employed to record the surface strain vs time associated with the wave. The duration of loading, which is equal to the time for the torsion wave to propagate twice the distance from the specimen observation surface to the free end of the extender bar, was varied from test to test by varying the sum of the lengths of the specimen and extender bar. The torsional shear stress is linearly proportional to the radius. Therefore, the strain gauges on the cylindrical surface measured the strain associated with the maximum shear stress. The maximum shear stress was varied from test to test by varying the amplitude of the torsion wave. The displacements of dislocations for a test could be obtained for stresses ranging from zero to the maximum shear stress for that test.

Specimen Bonding Techniques

Techniques for bonding the test specimen to the gauge and extender bars were developed for each test temperature, so that (i) the processes of bonding and unbonding without the intervening application of a torsion pulse did not produce detectable dislocation displacement, and (ii) the bonds transmitted the torsion wave without excessive decrease in amplitude or increase in rise time.

The bond for room temperature tests was made with

[5] A. P. L. Turner, T. Vreeland, Jr., and D. P. Pope, Acta Cryst. (to be published).

[6] D. P. Pope, T. Vreeland, Jr., and D. S. Wood, Rev. Sci. Instr. **35**, 1351 (1964).

a wax having a melting temperature of 75°C. Bonds for low-temperature tests were made with mixtures of glycerin and ethanol. Three parts glycerin to two parts ethanol was used at −100°C, and one part glycerin to five parts ethanol was used at −150°C. The bonds for the 70°C tests were made using a 120°C melting-temperature wax filled with levigated alumina powder. It was found that bonds in the order of 0.005 cm thick made with these materials would pass the torsion waves satisfactorily at the test temperatures.

Temperature Control and Measurement

The temperature was controlled during low-temperature tests by controlling the rate and temperature of cooled nitrogen gas flowing by the specimen. The temperature was measured using thermocouples attached to the gauge bar and shielded from the cold nitrogen gas by a rubber sleeve. Trial runs with a second thermocouple attached to a dummy specimen demonstrated that the gauge bar and specimen temperatures agreed within 2°C.

Temperature was controlled during the 70°C tests by varying the temperature of an isothermal glycerin bath. Trial runs showed that the glycerin and specimen temperatures agreed within 2°C.

The overall accuracy of the temperature control is estimated to have been ±5°C.

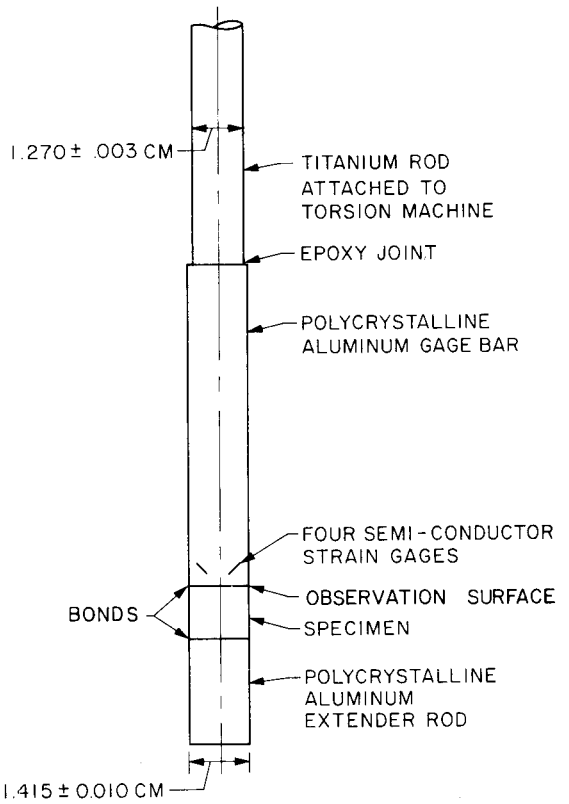

FIG. 1. Specimen and extender bonded to torsion machine.

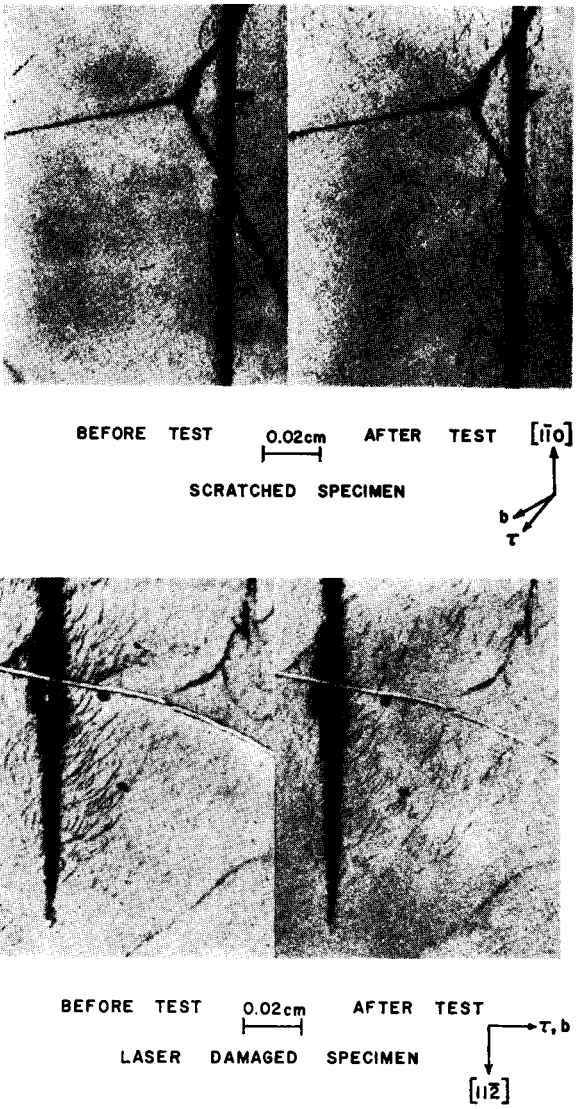

FIG. 2. Berg–Barrett x-ray micrographs showing dislocations before and after torsion tests.

Experimental Procedure

Three or more tests were run at temperatures of 70°, 23°, −100° and −150°C. The maximum shear stress at the outer edge of the specimens varied from 0.43 to 2.16×10^7 dyn/cm^2. The combined lengths of the specimens and polycrystalline aluminum extender rods were such that the load duration at the observation surface of the specimen ranged from 15 to 108 μsec.

EXPERIMENTAL RESULTS

Dislocation Displacement Measurements

Figure 2 contains enlargements of Berg–Barrett x-ray micrographs showing dislocation positions before and after torsion testing for a scratched specimen and for a laser-damaged specimen. The maximum displacement

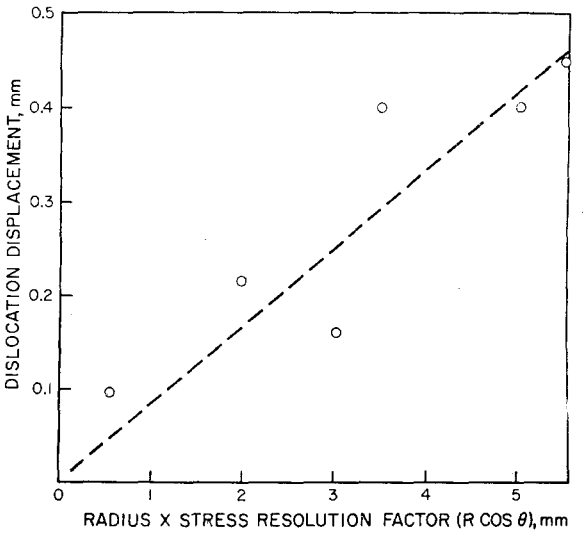

FIG. 3. Dislocation displacement vs product of radius and stress resolution factor for a typical test.

of dislocations during the test was measured on the Berg–Barrett x-ray micrographs using a microscope fitted with a calibrated filar eye piece. Each location along a scratch or line of laser damage where dislocation displacement reached a maximum provided a data point. The measurements were made where the dislocations were not impeded by subgrains and where the "after-test" dislocations were not tangled, i.e., where the leading dislocation was free of entanglement for a length of 0.1 mm or more. Therefore, the dislocation velocities calculated from these measurements are the maximum values for all dislocations which were observed to move at a given temperature and stress. The displacements measured from the micrograph were used directly in calculating the dislocation velocity, since the maximum error in distances on the micrographs relative to actual distances in the crystal was calculated to be less than five percent.

It can be seen from Fig. 2 that the dislocations moved out from only one side of the scratch or laser damage. This occurs since the scratching or laser damage produces dislocations of the same sign on both sides. (The forces due to scratching or laser-induced thermal expansion tend to produce dislocations with extra planes on the surface side of the dislocation slip plane.) The applied shear stress during the torsion test tends to return the dislocations on one side to the scratch or laser damage, while it tends to move those on the other side away from the scratch or laser damage. There were occasional instances of dislocations moving in both directions, showing that some dislocations of the opposite sign were produced.

The dislocation displacements observed in a typical test are plotted in Fig. 3 as a function of the product of the radius, R, and the stress resolution factor, $\cos\theta$, where θ is the angle between the tangential direction and the Burgers vector. The approximately linear trend of the data in Fig. 3 shows that the dislocation velocity is approximately linearly proportional to the resolved shear stress.

Stress and Time Measurements

Figure 4 shows tracings made from typical strain-gauge records, both for a torsion test with no specimen or extender attached to the gauge bar and for a torsion test with a specimen and extender attached. As shown in Fig. 4(a), a stress pulse without a specimen or lower extender rod attached had a short duration, corresponding to the time taken for the stress wave to pass the gauges, to be reflected from the free end to the gauge bar as an unloading wave, and to return to the gauges. As shown in Fig. 4(b), the stress pulse duration was increased by attaching a specimen and extender to the gauge bar. The additional area of stress pulse, marked A in Fig. 4(b), is the portion of the stress pulse due to the stress wave traveling down and back through the specimen and extender, and gives the stress-time history at the observation surface.

The maximum stress, τ_{max}, was taken from the pulse record. The numerical value of this maximum stress was obtained by comparison with previous tests run with dummy polycrystalline aluminum specimens and rigid bonds, in which the maximum stress for a strain-gauge reading was determined from the static torque applied to the torsion machine as described by Greenman *et al.*[1]

The resolved shear stress acting on a dislocation was obtained by using the relation $\tau=\tau_{max}(R/a)\cos\theta$, where R is the distance from the center of the specimen, a is the specimen radius, and θ is the angle between the tangential direction and the Burgers vector of the dislocation. The Burgers vector was determined from the

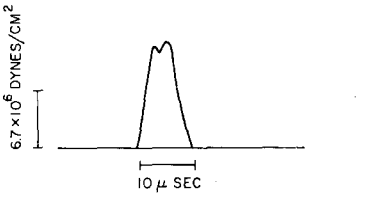

a RECORD OF TORSION STRESS PULSE WITH GAGE BAR ALONE.

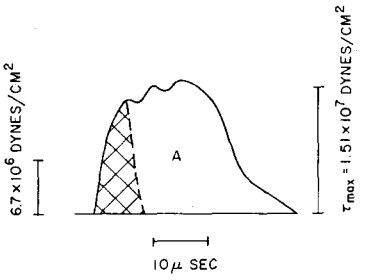

b RECORD OF TORSION STRESS PULSE WITH SPECIMEN AND EXTENDER. CROSS-HATCHED AREA DUE TO GAGE BAR ALONE.

FIG. 4. Strain gauge records of torsion stress pulses.

Berg–Barrett x-ray micrographs, as discussed previously. The above relation for resolved shear stress was not corrected for anisotropic effects since calculations showed that elastic anisotropy introduced a stress perturbation of less than 10%.

Dislocation Velocities

Dislocation velocities were calculated by dividing the measured dislocation displacement due to the load pulse by the pulse duration. The dislocation velocity data are plotted as a function of resolved shear stress for each temperature in Fig. 5. The data for each temperature are represented by a straight line from the origin through a point obtained by averaging all the stress-velocity data for that temperature. These data show that (i) the dislocation velocity is approximately linearly proportional to the applied-resolved shear stress, and (ii) the dislocation velocity decreases with increasing temperature for a given stress.

The linear relation between dislocation velocity and applied-resolved shear stress at any given temperature may be described by means of a viscous drag coefficient,

$$B=\tau b/v, \qquad (1)$$

which is the ratio of the drag force acting on a unit length of the dislocation to the dislocation velocity.

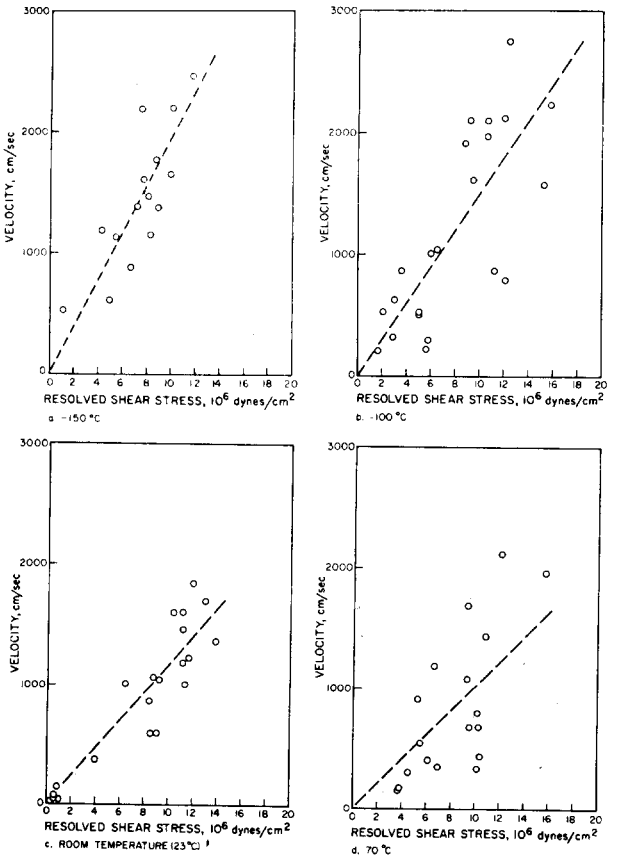

FIG. 5. Dislocation velocity vs applied-resolved shear stress.

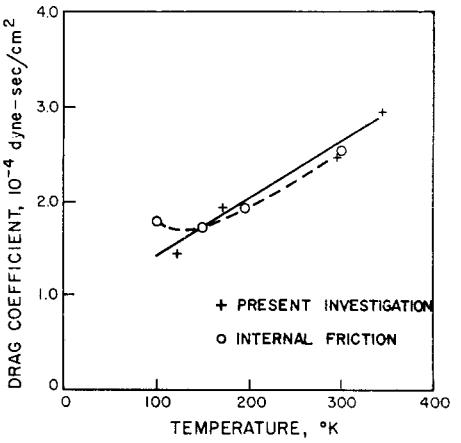

FIG. 6. Dislocation drag coefficient vs temperature.

Values of this drag coefficient obtained from the data given in Fig. 5 are plotted as a function of the absolute temperature in Fig. 6.

DISCUSSION

Effect of Line Tension

The line tension of a dislocation can reduce the net force on the dislocation if the dislocation is curved. A typical radius of curvature of the dislocations in a tested specimen is 0.03 cm. The stress required to maintain this radius is about 0.2×10^6 dyn/cm^2. The typical visible length of segments of dislocation line in the Berg–Barrett x-ray micrographs was 0.02 cm. At the locations where the dislocation becomes invisible, the dislocation line might continue at right angles to the visible segment. This would produce a retarding force, which would balance an applied stress of about 0.7×10^6 dyn/cm^2. Thus the stresses due to line tension were small compared to the applied stresses in this investigation, and it is concluded that the effect of line tension was negligible.

Effect of Dislocation Interactions

The stress fields of nearby dislocations on the same slip plane can change the effective stress acting on a dislocation. The dislocation furthest from the scratch or line of laser damage was typically about 0.002 cm from the nearest dislocation, both before and after testing. Assuming that the dislocations lie on the same slip plane and are edge dislocations, the interaction stress would be about 0.8×10^6 dyn/cm^2. This is a small stress compared to the applied stress for most data points; therefore, dislocation-interaction effects are believed to be small.

Effect of Pinning by Point Defects and Dislocations on Other Slip Planes

The effects of point defects and dislocations on other slip planes cannot be quantitatively assessed, and may

have contributed significantly to the scatter in the data shown in Fig. 5. The number of point defects was minimized by the use of 99.999 percent pure material. Diffusion of point defects to dislocations produced by scratches or laser damage is believed to be small, since delays varying between one hour and four days between producing the dislocations and torsion testing did not appear to affect the number of dislocations moving or their speed. The effect of dislocations on other slip systems is also believed to be small. Essentially all dislocations in the crystals close enough to the surface to affect the observed dislocations were coalesced into subgrain boundaries by annealing. This was confirmed in several cases by electrolytically removing about 50 μ of material from the surface of an annealed crystal and observing the dislocations as revealed in Berg–Barrett x-ray micrographs.

Acceleration Times

The method used to obtain dislocation velocities from the displacement and time-duration data assumed that the dislocation motion was in phase with the applied stress. This assumption is reasonable if the dislocation acceleration time is small compared to the stress-pulse rise time of about 2×10^{-6} sec. The effective mass m per unit length of a dislocation is about

$$m=(Gb^2)/C^2, \tag{2}$$

where G is the modulus of rigidity, and C is the shear wave velocity which equals $(G/\rho)^{1/2}$ where ρ is the mass density. The equation of motion for a dislocation then is

$$m(\partial v/\partial t)=\tau b-Bv. \tag{3}$$

Solving for v, one obtains

$$v=(\tau b/B)[1-\exp(-Bt/m)]. \tag{4}$$

The acceleration time constant is thus m/B, which for this experiment is on the order of 10^{-11} sec. This shows that the acceleration time is negligible, and thus that the dislocation velocity was essentially in phase with the applied stress during the applied stress pulses used in this investigation.

Comparison with Other Experimental Results

The drag coefficient B for dislocation velocity has been measured by two other techniques: internal friction tests,[7] and impact shear tests.[8] The results obtained from internal friction measurements are shown in Fig. 7, and are seen to be an order of magnitude larger than the values obtained in the present investigation. As noted by Mason and Rosenberg,[7] the internal friction measurements actually determine the ratio B/ρ_m, where ρ_m is the density of mobile dislocations. The experimental values of B shown in Fig. 7 were based on an assumed density of mobile dislocations of 8×10^6 cm/cm^3. The internal friction results can readily be brought into agreement with the results of the present investigation by assuming a smaller value for the density of mobile dislocations during the internal friction measurements. The temperature dependence of the dislocation drag coefficient determined by the internal friction measurements agrees quite well with the results of the present investigation as shown in Fig. 6. The values of B from the internal friction measurements shown in Fig. 6 were obtained by using a value for ρ_m of 1.23×10^6 cm/cm^3 rather than 8×10^6 cm/cm^3 as assumed by Mason and Rosenberg.

In the impact shear tests,[8] strain rate is measured as a function of shear stress. Determining a value for the drag coefficient, B, from the shear stress-strain rate data requires that a value be assumed for the unknown density of mobile dislocations, ρ_m. The values of B determined from the impact tests are nearly an order of magnitude greater than those determined from the present experiments. Also, they show the opposite temperature dependence when compared to the results of this experiment and the internal friction tests cited previously. The magnitude difference in B can be attributed to the unknown value of ρ_m. The opposite temperature dependence, as discussed by Ferguson *et al.*,[8] may be due to dislocations in the shear impact tests interacting with other dislocations or impurities. In addition, the value of ρ_m could vary with temperature, stress, strain, or strain rate, and confuse the analysis of the data; for example, a fairly small decrease in ρ_m as temperature is decreased would reverse the temperature dependence of B. It is concluded that the drag coefficient determined by the impact shear tests is not applicable to individual dislocations interacting with the lattice.

Comparison with Theoretical Mechanisms Governing Dislocation Velocities

The theoretical mechanisms governing the velocity of dislocations in relatively pure materials can be divided into two groups, i.e., mechanisms which do and do not involve a thermal activation process. In the theories involving thermally activated processes, dislocation velocity is considered to be governed by the time required for thermal fluctuations to assist the dislocation to overcome some barrier to its motion, such as interactions of dislocations with point defects,[9,10] Peierls barriers,[11] and forest dislocations.[12] All such theories predict that the dislocation velocity should increase rapidly with increasing temperature. A thermal

[7] W. P. Mason and A. Rosenberg, Phys. Rev. **151,** 434 (1966).
[8] W. G. Ferguson, A. Kumar, and J. E. Dorn, J. Appl. Phys. **38,** 1863 (1967).
[9] J. J. Gilman, J. Appl. Phys. **36,** 3195 (1965).
[10] R. L. Fleischer, J. Appl. Phys. **33,** 3504 (1962).
[11] J. E. Dorn and S. Rajnak, Trans. AIME **230,** 1052 (1964).
[12] A. Seeger, S. Mader, and H. Kronmüller, *Electron Microscopy and Strength of Crystals* (Interscience Publishers, Inc., New York, 1963), p. 665.

activation process clearly does not control dislocation velocity in high-purity-aluminum single crystals under the conditions of the present experiments, since the dislocation velocity is found to decrease with increasing temperature.

The proposed mechanisms governing dislocation velocity in pure, highly perfect single crystals which do not depend on thermal activation involve the interaction of dislocations with lattice thermal vibrations (phonon drag) or with electrons (electron viscosity), or are based on relaxation effects in the dislocation core (glide-plane viscosity). There has been considerable speculation as to whether the various phonon-drag mechanisms, (i) phonon viscosity,[13–15] (ii) thermoelastic effects,[16,17] (iii) anharmonic radiation from the dislocation core,[18] and (iv) phonon scattering,[18] are really different mechanisms or merely different ways of looking at the same mechanism. The authors feel that the various phonon-drag mechanisms are different, since they appear to be based on different physical processes. In particular, phonon viscosity and phonon scattering appear to be different, since phonon viscosity arises from a departure from thermal equilibrium of the phonon modes, while phonon scattering does not involve any departure from thermal equilibrium. The phonon-drag mechanisms, together with the electron viscosity[19,20] and glide plane viscosity[21] mechanisms, are briefly described below.

Phonon Viscosity

The phonon viscosity theory developed by Mason[13–15] may be summarized as follows. A shear stress can be resolved into a compressive stress and an orthogonal tension stress. If a step change in shear stress is impressed on a region of a crystal, the radiation pressure of the phonon gas in the compression direction is increased with a corresponding increase in phonon temperature, while the radiation pressure and temperature are decreased in the tension direction. These changes in radiation pressure cause an increase in the modulus of rigidity of $E_0/3$, where E_0 is the thermal-energy density. The increase in the modulus relaxes with a characteristic time determined by the rate at which phonons of different modes approach quilibrium, i.e., the rate at which the different phonon modes approach the same temperature. This relaxation effect can cause the stress and strain in a crystal due to motion of a dislocation to be out of phase and thus result in dissipation of energy and damping of the dislocation motion.

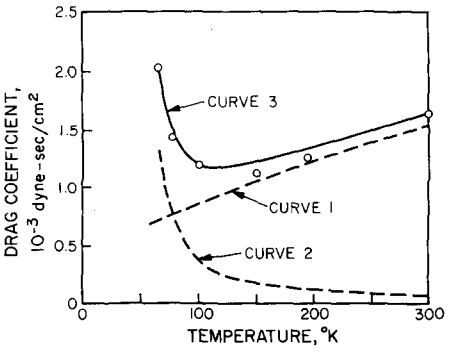

o EXPERIMENTAL VALUES
CURVE 1 - THEORETICAL PHONON VISCOSITY
CURVE 2 - THEORETICAL ELECTRON VISCOSITY
CURVE 3 - SUM OF PHONON AND ELECTRON VISCOSITIES

FIG. 7. Dislocation drag coefficient vs temperature from internal friction measurements and theories, see Ref. 7.

This theory predicts that the dislocation velocity is linearly proportional to the applied-resolved shear stress, which is in agreement with the results of the present investigation. Mason[15] obtains for the dislocation-drag coefficient due to phonon viscosity:

$$B=b^2DE_0K/8\pi a_0^2C_v\bar{V}^2, \tag{5}$$

where D is an elastic nonlinearity constant, K is the lattice thermal conductivity, a_0 is the dislocation core radius, C_v is the specific heat per unit volume, and $\bar{V}$ is the mean phonon velocity. According to Mason and Bateman,[14] the value for the nonlinearity constant can be calculated if the third-order elastic constants are known. For aluminum, the third-order elastic constants are not known and the nonlinearity constant has not been evaluated. Mason and Rosenberg[7] estimate that a value of $D=3.95$ is necessary to make theoretical values of dislocation damping fit their internal friction data. However, since this fit also depends on their assumed values for dislocation density and dislocation core radius, the value of the nonlinearity constant for aluminum remains uncertain. Equation (5) for the drag coefficient is also uncertain because of the difficulty of determining the proper values of the dislocation core radius and the lattice thermal conductivity. Mason[13] originally used a core radius of $a_0=b/6$, but subsequently[15] recommended using $a_0=\frac{3}{4}b$ or $a_0=v/\Delta t$, whichever was larger, where v is the dislocation velocity, and Δt is the phonon relaxation time given by:

$$\Delta t=\bar{l}/\bar{V}=3K/C_v\bar{V}^2, \tag{6}$$

where $\bar{l}$ is the phonon mean free path. The value of $a_0=\frac{3}{4}b$ is justified by Mason on the basis that it is the limit to which linear elasticity theory holds, and $a_0=v/\Delta t$ is justified on the basis that for a radius less than $v/\Delta t$, phonon relaxation will not occur during the transit time of the dislocation core. Under the conditions of

[13] W. P. Mason, J. Acoust. Soc. Am. **32,** 458 (1960).
[14] W. P. Mason and T. B. Bateman, J. Acoust. Soc. Am. **36,** 644 (1964).
[15] W. P. Mason, J. Appl. Phys. **35,** 2779 (1964).
[16] J. D. Eshelby, Proc. Roy. Soc. (London) **A197,** 396 (1949).
[17] J. H. Weiner, J. Appl. Phys. **29,** 1305 (1958).
[18] J. Lothe, J. Appl. Phys. **33,** 2116 (1962).
[19] W. P. Mason, *Physical Acoustics and The Properties of Solids* (D. Van Nostrand Co., Inc., Princeton, New Jersey, 1958), p. 323.
[20] W. P. Mason, Appl. Phys. Letters **6,** 111 (1965).
[21] J. J. Gilman, Phys. Rev. Letters **20,** 157 (1968).

this experiment, $\frac{3}{4}b > v/\Delta t$, so a_0 is taken to be $\frac{3}{4}b$. On the other hand, Lothe[18] considers that $\bar{l}$, the phonon mean free path, should be used as the core radius.

If Mason's choice of the core radius or any other constant core radius is used, the temperature dependence of the drag coefficient given by (5) is determined by the variation of E_0, K, and C_v with temperature. If Lothe's[18] choice of the core radius is used, the value of the drag coefficient becomes, using Eq. (6) for $\bar{l}$,

$$B = b^2 D E_0 C_v / 72\pi K, \tag{7}$$

which shows a much more rapid fall off with temperature than if a constant core radius is used, because C_v decreases and K increases as temperature is decreased.

The temperature dependence of the drag coefficient, calculated using a constant dislocation core radius, agrees fairly well with the results of this experiment. However, the magnitude of the drag coefficient calculated by Mason and Rosenberg,[7] using a core radius of $a_0 = \frac{3}{4}b$ and a nonlinearity constant $D = 3.95$, is about six times greater than that measured in this experiment. Their theoretical results, using $a_0 = \frac{3}{4}b$ and $D = 3.95$, are shown in Fig. 7. Thus the results of the present experiments indicate that in the phonon viscosity theory a constant core radius should be used, but that the value of the core radius must be increased, and possibly the nonlinearity constant must also be decreased in order to bring theory and experiment into agreement.

Thermoelastic Effect

Eshelby[16] demonstrated that the compressive and tensile stresses around a moving edge dislocation will cause irreversible heat flow to take place and thus will dissipate energy. Calculations using the equations of Weiner[17] and Lothe[18] show that this effect results in a drag coefficient for aluminum three or more orders of magnitude less than that determined in this experiment. The low rate of energy dissipation in aluminum due to this effect is a result of the high thermal conductivity of aluminum, which makes the compression and tension around the edge dislocation occur in a nearly isothermal manner.

Anharmonic Radiation from the Dislocation Core

The vibrational energy of the atoms in the highly distorted region of the dislocation core is increased when the dislocation moves due to the anharmonic coupling forces between atoms. The radiation of this energy away from the dislocation contributes to dislocation damping. Lothe[18] has estimated the effect of anharmonic radiation for an edge dislocation and obtained

$$B = E_0 b / 12\bar{V}. \tag{8}$$

Equation (8) is uncertain because of the difficulty of estimating the vibrational frequency and energy changes that occur in the dislocation core. Equation (8) gives a value of the drag coefficient at room temperature about an order of magnitude lower than that measured in this experiment. In addition, the value of the drag coefficient given by Eq. (8) decreases more rapidly as temperature decreases than does the experimental drag coefficient.

Phonon Scattering

The various mechanisms by which dislocation damping can be caused by phonon scattering have been reviewed by Lothe.[18] At temperatures below the Debye temperature for materials with a negligible Peierls barrier, such as aluminum, there are two significant phonon scattering mechanisms. The first mechanism is the scattering of phonons by the dislocation strain field in a manner analogous to the refraction of light. The second mechanism is the absorption of energy from phonons by the dislocation and subsequent vibration of the dislocations with reradiation of phonons. Lothe[18] finds that the drag coefficient from strain-field scattering will be in the range

$$(E_0 b/60\bar{V}) < B < (E_0 b/5\bar{V}), \tag{9}$$

and that the drag coefficient due to induced vibrations is

$$B \approx E_0 b/10\bar{V}. \tag{10}$$

The drag coefficient from both types of phonon scattering is then about:

$$B \approx E_0 b/5\bar{V}. \tag{11}$$

The magnitude of this drag coefficient at room temperature is about one fourth of the experimental value, and it decreases with decreasing temperature more rapidly than the experimental value.

Electron Viscosity

The free electron gas in a metal can cause viscous damping of dislocation motion in the same manner as discussed above for the phonon gas.[19,20] The value of the dislocation drag coefficient again is uncertain because of uncertainty in the proper value of the core radius. Mason and Rosenberg[7] have computed the drag due to electron viscosity as a function of temperature with the assumption that the core radius is about 10^{-7} cm. Their results are shown in Fig. 7 together with data from internal friction measurements. The theoretical results indicate that below 100°K, the effects of electron viscosity on the drag coefficient should become noticeable. The present experiment did not reach a sufficiently low temperature to test that prediction.

Glide-Plane Viscosity

Gilman[21] has proposed that the dislocation-drag coefficient is primarily due to viscous effects in the dislocation core, which are neglected by Mason and Rosenberg. He estimates that the viscous losses in the core

region exceed those in the bulk of the crystal by a factor of about eight. Gilman suggests that the value of viscosity η computed by Mason using the phonon-viscosity theory is the appropriate value to employ for for metals in his expression for the drag coefficient B.

A quantitative analysis of glide-plane viscosity cannot be performed, since there is as yet no way of estimating an appropriate value of the viscosity. Phonon viscosity probably is not applicable to the dislocation core, since phonon viscosity depends on phonon–phonon interactions and, therefore, is not applicable to regions much smaller than the phonons mean free path. Also, if the phonon-viscosity value of η were used in Gilman's theory, it would result in a drag coefficient B about 50 times greater than that obtained in the present investigation.

This comparison of theory with the results of the present experiment indicates that the thermoelastic effect is negligible compared to the other mechanisms, and that the glide-plane viscosity theory is difficult to evaluate quantitatively, but tentatively appears to predict too large a dislocation damping. The electron-viscosity mechanism may contribute to the low-temperature damping; however, the magnitude of the effect was too low to be detected in the test temperature range of the present investigation. Anharmonic radiation and phonon scattering may contribute significantly to dislocation damping at high temperatures (room temperature and above), but phonon viscosity appears to be the predominant damping mechanism governing the mobility of glide dislocations on the (111) planes in aluminum in the temperature range $-150°$ to 70°C. This conclusion is based on the temperature dependence of the theories when compared to the results of the present experiment, as shown in Fig. 8. Figure 8 shows the dislocation-drag coefficient B as a function of absolute temperature, as determined by

(a) results of the present experiment;

(b) phonon-viscosity theory, using values for the nonlinearity constant and core radius selected to give a good fit with the results of this experiment;

(c) phonon scattering and anharmonic radiation theory, with constants selected to give agreement with the results of this experiment at 350°K.

Figure 8 shows that the drag coefficients B from the phonon-viscosity theory and the experimental results have about the same temperature dependence, while the drag coefficient from the phonon-scattering and anharmonic-radiation theory decreases too rapidly as temperature is decreased. Electron viscosity effects, if added to the phonon-scattering and anharmonic-radiation results, are not sufficiently great to correct the temperature dependence discrepancy of the phonon-scattering theory. Significance should not be attached to the agreement in the mganitude of the drag coefficients shown in Fig. 8, since the constants used in the theories were arbitrarily selected.

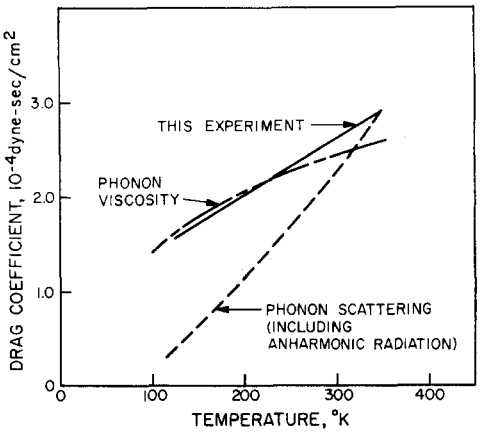

FIG. 8. Theoretical and experimental dislocation drag coefficients vs temperature.

SUMMARY AND CONCLUSIONS

Dislocations of edge and mixed character were produced within a depth of about 10μ below the (111) test surface of 99.999% purity-aluminum single crystals by scratching and by damaging with laser pulses. Movement of these dislocations on the (111) glide planes parallel to the observation surface was produced by resolved-shear stresses ranging from 0.5 to 16×10^6 dyn/cm^2 applied to the observation surface for periods ranging from 15 to 108 μsec. Tests were performed in the temperature range $-150°$ to 70°C. Dislocation displacement was measured using the Berg–Barrett x-ray technique.

Dislocation velocity determined from the test data at each test temperature was approximately linearly proportional to the applied-resolved shear stress. Dislocation velocity increased as temperature decreased at the same stress. The dislocation-drag coefficient ranged from 1.5×10^{-4} dyn·sec/cm^2 at $-150°$C to 2.9×10^{-4} dyn·sec/cm^2 at 70°C. The variation of dislocation velocity with stress and with temperature agrees approximately with the predictions of the phonon-viscosity theory.[7,13,15] The theory predicts somewhat lower velocities than those observed, however. This discrepancy may result from uncertainty in the appropriate dislocation core radius and nonlinearity constant to use in the theory. Phonon scattering and anharmonic radiation of phonons from the dislocation core[18] may also contribute significantly to limiting dislocation velocity, particularly in the higher-temperature portion of the test range. The glide-plane viscosity theory[21] predicts dislocation velocities much lower than those observed, and thus does not appear to be the mechanism governing dislocation velocity under the conditions of the present investigation.